Materials Research Proceedings 28 (2023) 437-444 https://doi.org/10.21741/9781644902479-48

Electron backscatter diffraction (EBSD) as a tool for analysis of metal flow in aluminum extrusion

PIRES Michael V.[1,a *], MADURA Jacek[2,b], MISIOLEK Wojciech Z.[1,c]
LEŚNIAK Dariusz[2,d], ZASADZIŃSKI Józef[2,e] and JURCZAK Henryk[3,f]

[1]Loewy Institute, Lehigh University, Bethlehem, PA, USA

[2]AGH University of Science and Technology, Krakow, Poland

[3]Albatros Aluminium, Wałcz, Poland

[a]mvp217@lehigh.edu, [b]madura@agh.edu.pl, [c]wzm2@lehigh.edu, [d]dlesniak@agh.edu.pl, [e]zas@agh.edu.pl, [f]h.jurczak@albatros-aluminium.com

Keywords: EBSD Technique, Porthole Dies, Aluminum Extrusion

Abstract. Electron backscatter diffraction was used to analyze the crystallographic texture within extruded AA6005 hollow profiles, allowing for the analysis of metal flow through various extrusion porthole die designs of different metal deformation conditions. Control of metal flow through a die design is necessary to meet industry demands for faster-running dies, tighter tolerances, thinner walls, and reduced extrusion loads. A standard die was compared with an innovative die design that doubled the extrusion exit speed. Analysis of metal flow was performed to provide additional insight into the uniformity of the metal flow, especially near the extrusion welds. Finite element method simulations were performed to predict the die exit temperature and plastic strain distributions. Local texture varied across the core and surface regions of the tube wall but remained consistent between both extrudates. A peripheral coarse grain structure was found within both extrudates, due to their elevated exit die temperatures.

Introduction

The purpose of this work is to develop a quality control tool, which can analyze the homogeneity of an extrudate's microstructure and local crystallographic texture for an innovative porthole die design that allows for the minimization of the resistance to deformation. This translates into increasing the efficiency of the extrusion production process in the area of forming limit diagrams. A die design that ensures optimal metal flow translates into an increase in the flow rate in the connection with the load capacity of the press. An optimal die design also provides a reduction in the extrusion force, which is beneficial from the point of view of energy balance and die strength [1]. For these reasons, testing is required to determine the dies' effectiveness. Finite element method (FEM) numerical simulations as well as metallurgical characterization techniques may be utilized to predict and determine part properties. In this study, a standard porthole die design was compared to a new innovative porthole die design with increased extrusion exit speed in an attempt to increase production during the extrusion process. FEM numerical calculations were performed using QForm UK Extrusion software. The extrusion model is based on the Lagrange-Eulerian approach, which included coupled simulations of the material flow and die deflection during the process [2]. The approach uses a proprietary material model of a deformed aluminum alloy developed based on a high-temperature compression test on a Gleeble 3800 metallurgical process simulator. Simulations of different variants of dies were carried out under identical process parameters, including heating the billet to 480ºC. FEM numerical calculations were performed to predict both the exit temperature and plastic strain distribution throughout the extrudate cross sections but still requires validation through experimental data.

Content from this work may be used under the terms of the Creative Commons Attribution 3.0 license. Any further distribution of this work must maintain attribution to the author(s) and the title of the work, journal citation and DOI. Published under license by Materials Research Forum LLC.

Electron Backscatter Diffraction (EBSD) was utilized as the experimental method of choice to characterize the localized microstructural texture and average grain size within the resultant extrudates, as a result of their deformation conditions. Election backscatter diffraction, or backscatter Kikuchi diffraction, is a scanning electron microscope (SEM) based technique that can be used to determine local microstructural texture, generally associated with the crystallographic orientation of individual grains within a material. This allows for microstructure reconstruction and detailed characterization of the microstructural properties of a material [3]. EBSD utilizes automated Kikuchi pattern indexing software to determine the orientation of multiple grains at once, making it a fast and accurate method for generating large quantities of data. Indexing of patterns involves the identification of individual (Kikuchi) bands based on the presence or absence of specific crystallographic poles (zone axes) as well as bandwidth [4, 5]. It is important to define the notation of the extrudate axes to better describe the areas of interest for the EBSD analysis, which is shown in Fig. 1, below.

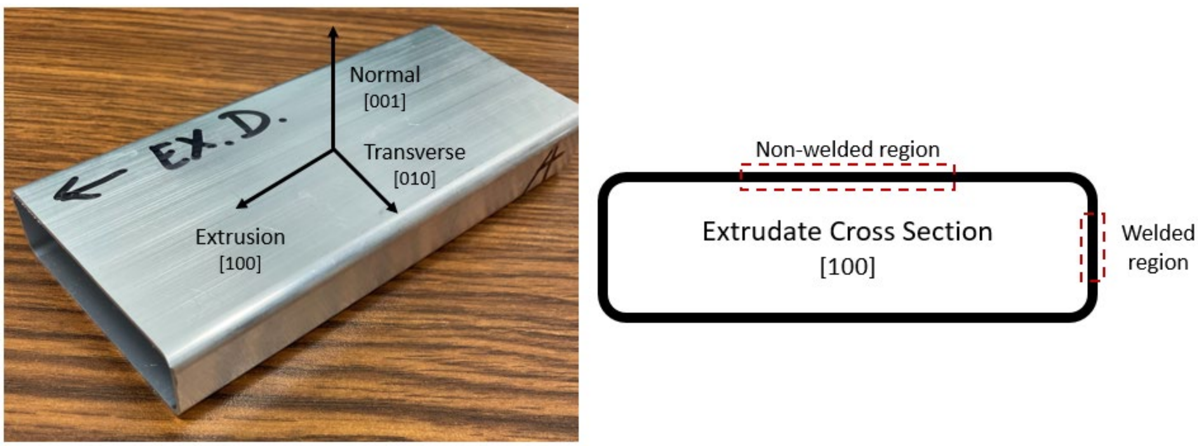

Fig. 1. Example of extrudate direction notation and regions of interest.

It is expected to obtain a homogenous microstructure within the extrudate as a result of die design, and therefore, altering deformation conditions. EBSD, as a proposed modern tool for metal flow analysis, will help to indirectly verify these results and the FEM predictions of exit temperature and plastic strain distribution.

Experimental Procedure

The samples analyzed in this study were thin-walled extrudates from 7-inch AA6005 billets extruded on 17 MN hydraulic press. Two profiles, A and D, were developed and extruded at the same temperature within different two-cavity dies consisting of similar web designs. Thus, the localization of transverse welds was the same. Profile A consisted of a conventional die with a maximum extrusion exit speed of 24 m/min and a specified maximum ram load of 15.36 MN. Profile D consisted of a new die with an innovative design ensuring an almost doubled increase in the extrusion exit speed of 42 m/min. The construction ensured a reduced plastic flow resistance, which was indicated by a lower maximum extrusion load of 14.88 MN. Both extrudates were cooled on the press run-out table under forced air. The maximum extrusion speed was determined for each of the dies in industrial trials while maintaining the required product surface quality. The measurement of the extrudate extrusion exit speed corresponded to the puller speed on the runout table. This was measured by sensors and using press software. The maximum speed was determined by the force capabilities of the press with simultaneous control of the temperature and the quality of the extrudates surface.

Improved process parameters were the result of using an extrusion die with larger ports, increasing the volume of metal flow by 45%. Thin webs were also used to ensure an even metal flow to the welding chambers. Equal filling of the bearing took place using a special port with a dedicated geometry. The new die design was developed based on FEM numerical simulations of the extrusion process. In the extrusion process design for the hollow sections of aluminum alloys, the exact conditions required to occur on the bearing surface must be determined. This can be obtained by numerical analysis, which includes parameters such as plastic strain and temperature distributions [6]. The developed extrusion process ensured a slight die deflection but yielded a high dimensional accuracy of extrudates. Both numerical simulations and physical measurements confirmed this. The deflection in the core and bearings was the result of numerical simulations, which is an elastic deformation that translates into the geometric accuracy of extrudates. Physical measurements were carried out after the experiment, which confirmed no evidence of plastic deformation of the tooling.

To prepare for experimental characterization, the extrudates were sectioned using a Struers Accutom-50 high-speed abrasive cutoff blade and mounted in epoxy resin, set in a vacuum to remove air bubbles, and left to cure overnight. Samples were metallographically prepared to a 0.25 μm finish with diamond media on a Buehler AutoMet250 automatic polishing unit before a 0.05 μm finish with colloidal silica on a vibratory polisher. Samples were cleaned in an ultrasound bath with ethanol and airdried using high heat. Silver paint was applied to the surface of the sample and left to dry for a minimum of 12 hours to prevent the buildup of current on the sample surface within the electron microscope.

Electron backscatter diffraction (EBSD) was performed in an FEI SCIOS Focused Ion-Beam (FIB) unit. Data was generated using EDAX TEAM software and analyzed with TSL OIM v8 software. EBSD maps were rebuilt using NPAR and further cleaned to achieve higher accurate confidence indexing (CI > 0.2) throughout the area of interest. An accelerating voltage of 10 kV was used in combination with a current of 6.4 nA during image collection. Maps were taken with a maximum sampling grid of 1024 x 800 pixels, individually modified to reduce both the scan area and total collection time. Maps were generated using a step size between 3-4 μm, consisting of hexagonal pixels. The EBSD camera was optimized using an *Ultra-Fast* setting to acquire a maximum of 170 frames per second (fps) under the listed conditions.

Numerical Investigation

FEM numerical simulations of the exit temperature and plastic strain distributions were performed for both extrudates A & D. The areas of interest highlighted within a black box, shown in both Fig. 2 and 3, for both the *non-welded* and *welded* regions correspond to the fields of view discussed later in the *Results & Discussion* section, shown as EBSD maps in Fig. 4. The exit temperature simulations, shown in Fig. 2, exhibited a variation of 10 °C throughout the entire cross-section, but was consistent across the full wall thickness at any given point, within a single degree. Comparing both profiles, A & D, a maximum exit temperature of 550°C was recorded near the center of the *non-welded* regions, steadily decreasing to a minimum temperature of 540°C as the cross-sectional corners were approached. In respect to the *welded* regions, profiles A & D were again consistent amongst each other, but with opposing results at either side of the extrudate. For the purpose of this study, the area of interest was focused on the right side of the extrudate cross-section, with a recorded exit temperature of 550°C.

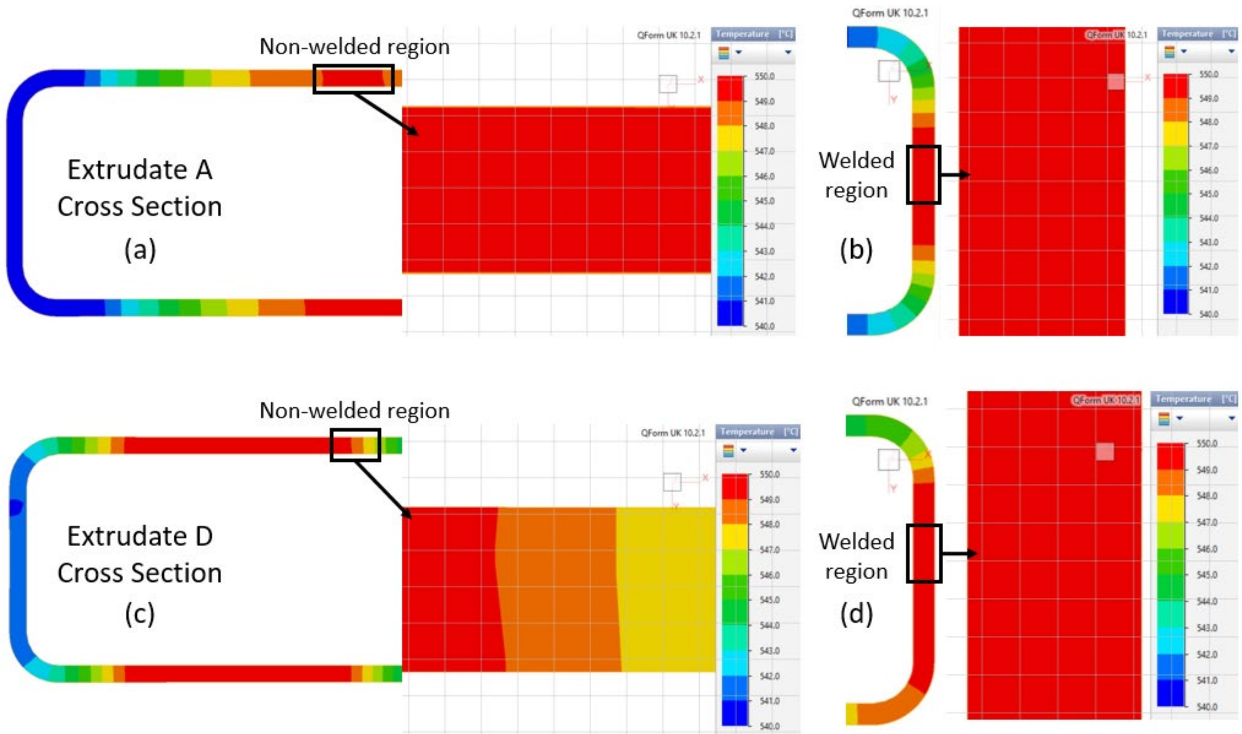

Fig. 2. FEM simulation of Exit Temperature for both Extrudate A (a, b) and Extrudate D (c, d).

The plastic strain simulations, shown in Fig. 3, exhibited a consistent strain gradient throughout the entire die other than at the center of both *welded* regions, including both sides of each extrudate. A minimum plastic strain, corresponding to the light blue color, was recorded at the center of the wall thickness where the least deformation is expected to occur. A gradient was recorded on either side of the wall thickness as the surface was approached, where the extrudate and die are in contact and the most deformation is expected to occur. The only discrepancy in the strain gradient occurred within the *welded* regions, where the localization of the longitudinal weld is believed to exist. Overall, the outer surface of the extrudate experienced a larger plastic strain compared to that of the inner surface, which was more apparent within the *welded* regions than within the *non-welded* regions. Upon closer inspection, a more balanced strain distribution across the wall thickness was revealed for profile A in the *non-welded* region, whereas a more balanced distribution was revealed for profile D in the *welded* region.

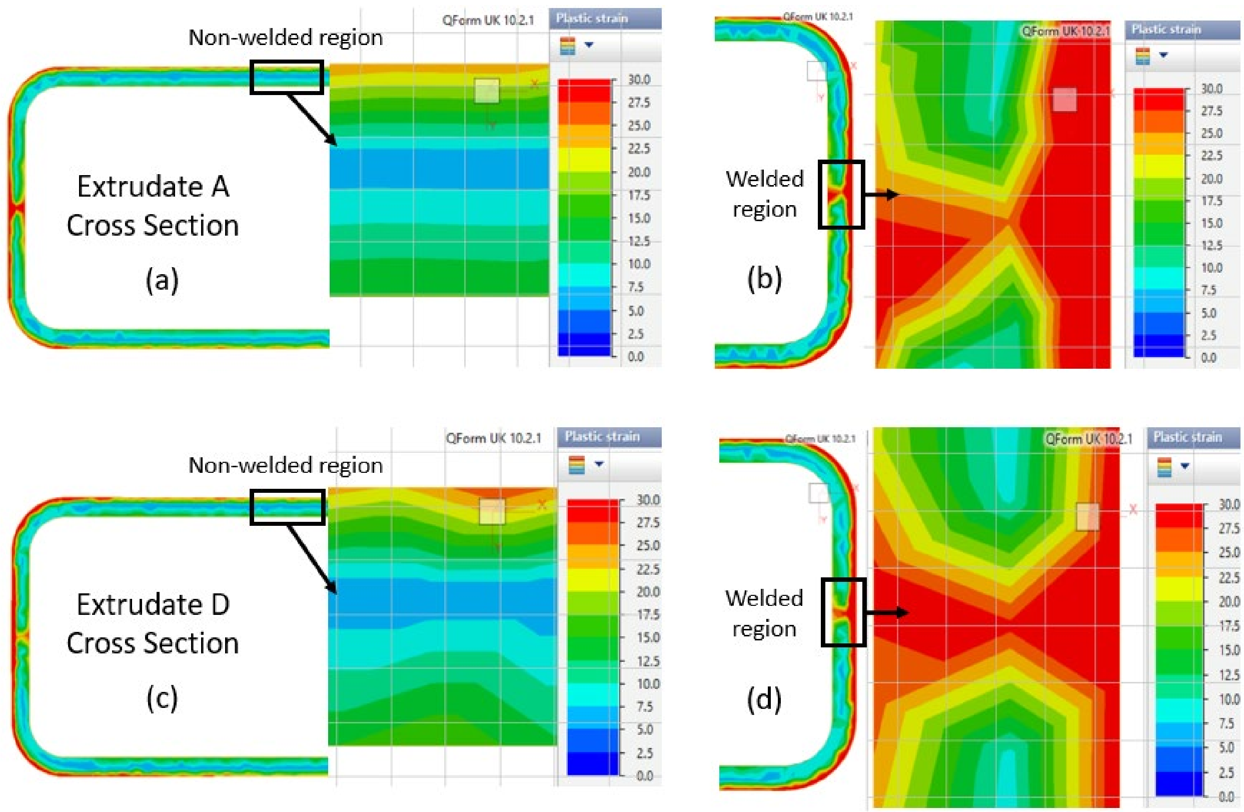

Fig. 3. FEM simulation of Plastic Strain for both Extrudate A (a, b) and Extrudate D (c, d).

Results and Discussion

Election backscatter diffraction was utilized to measure the microstructural texture and grain size of hot extruded AA6005 billets. A few considerations were made to generate accurate indexed patterns. As aluminum is a beam-sensitive material, a low accelerating voltage/beam current was necessary to reduce beam damage during mapping, which led to a loss in collection time and pattern quality. In addition, low magnification (80-100x) imaging was necessary to generate large enough fields of view for the regions of interest within the extruded samples. Below a magnification of ~250x, distortion of the image can occur due to a large focal plane when tilted at 70° for the EBSD technique. Using a low magnification can also make smaller grains difficult for the software to distinguish. A step (pixel) size of 3-4 µm was used to balance between pattern quality and collection time. The EDAX TEAM software incorporates Neighbor Pattern Averaging and Re-indexing (NPAR), which was used for post-process map rebuilding, greatly improving the accuracy of results and quality of the images presented in this study [7, 8].

Samples A and D were analyzed. EBSD maps of their areas of interest were generated, shown in Fig. 4. Throughout each field of view for both samples, the center of the extrudate exhibited a strong [001] texture corresponding to the color red/orange, whereas the surfaces in contact with the die transitioned into a [101] texture corresponding to the color green. In addition, a weak [111] texture corresponding to the color blue was recorded throughout the extrudate, but in larger amounts near the extrudate surface. The localized microstructure can be seen to vary from extrudate core to its surfaces due to different strain and friction conditions of the die. This result was to be expected and validated the plastic strain gradients recorded in the FEM simulations in Fig. 3.

Comparing the *non-welded* regions (Fig. 4a & 4c) the overall texture profile remained the same, but a decrease in average grain size from 95.6 µm to 83.7 µm occurred as the extrusion exit speed doubled. Within the *welded* regions (Fig. 4b & 4d) there was a drastic increase in average grain size from 66.5 µm to 82.8 µm. This increase in average size was likely a result of abnormal grain growth, occurring near the outer surface within extrudate D. It is necessary to state that microstructural imperfections are known to occur during hot extrusion of aluminum alloys, such as in this case, a peripheral coarse grain (PCG) structure. This was more evident within the *non-welded* regions, but existed for both profiles A & D. Eivani et. al. concluded that elevated temperatures above 500°C during extrusion could cause PCG to form [9]. The presence of a PCG structure within both profiles may validate the FEM simulations in Fig. 2, which recorded exit temperatures entirely above 540°C. Van Geertruyden et. al. concluded that PCG is likely the result of delayed recrystallization, forming within a few seconds after exiting the die at elevated temperatures. He also found that a lack of recrystallization-inhibiting elements, such as Cr, increased the depth of PCG within the AA6xxx extrudate [10]. The low alloying content of these AA6005 extrudates while also undergoing air-cooling suggested the presence of PCG was likely to occur.

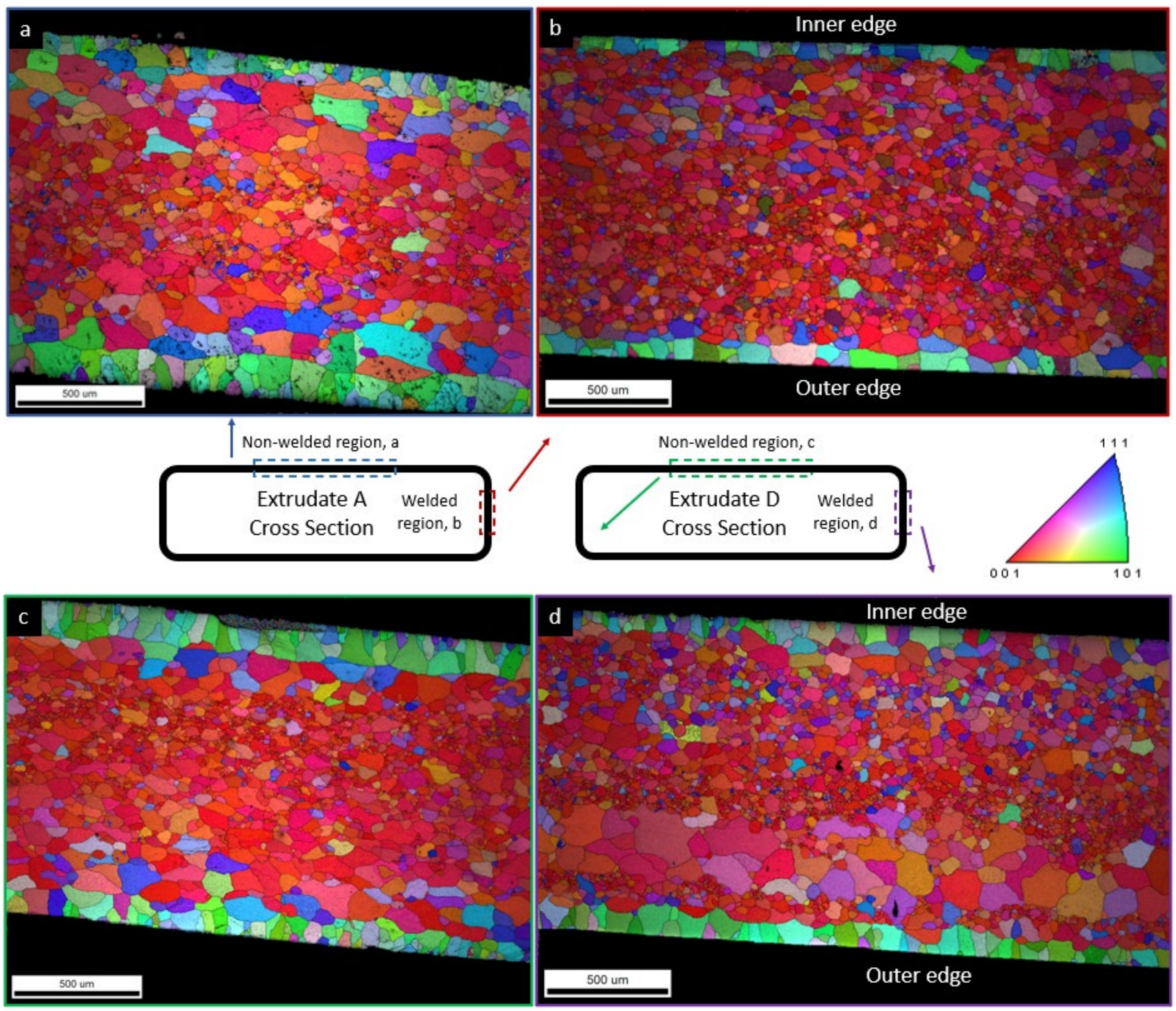

Fig. 4. EBSD crystallographic orientation maps of Extrudate A (a, b) and Extrudate D (c, d).

Inverse pole figures (IPFs) were generated for each region of interest corresponding to the extrusion [100], transverse [010], and normal [001] directions. These figures represent binary black-and-white intensity maps that relate to the area of points (in this case, grains) bound to a specific crystallographic direction. A higher intensity of dark area correlates to a stronger texture for any given plane. Fig. 5, shows the majority of grains were orientated towards both the <100>

Materials Research Proceedings 28 (2023) 437-444 https://doi.org/10.21741/9781644902479-48

and <110> family of planes along the extrusion [100] direction for both *non-welded and welded* regions between both extrudates. While along the transverse [010] direction, there was a weak or randomized texture as the intensity of points was spread homogeneously between the IPFs. Comparing each family of planes between all four areas of interest exhibited a consistent texture profile, implying that increasing the extrusion exit speed had little to no effect on the result of microstructural orientation.

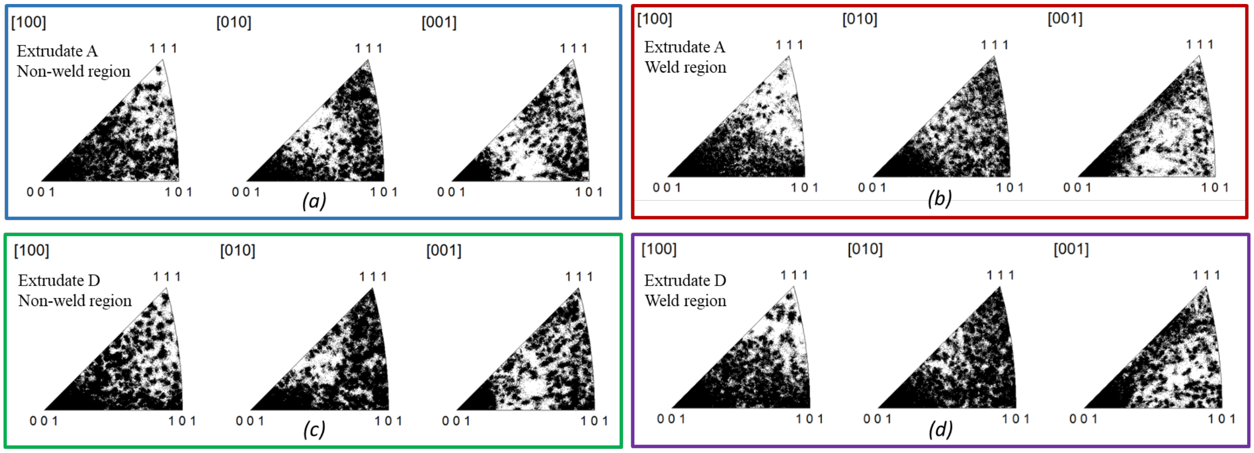

Fig. 5. Inverse pole figures for both Extrudate A (a, b) and Extrudate D (c, d).

Summary

Electron backscatter diffraction was utilized as a characterization method to analyze the localized microstructural texture, grain size, and metal flow of hot extruded AA6005 hollow profiles and to verify FEM predictions of exit temperature and plastic strain distribution. The average grain size decreased from 95.6 µm to 83.7 µm within the *non-welded* region and increased from 66.5 µm to 82.8 µm as the extrusion exit speed doubled. The increased grain size within the *welded* region was likely due to abnormal grain growth, but its cause was yet to be confirmed in this study. Similar die exit temperatures >500°C were recorded for both extrudates using the FEM simulations. Literature has shown this may have likely contributed to the PCG structure found throughout both extrudates. Local crystallographic texture varied across the core to surface, but remained consistent between both extrudates, with a strong [100] texture within the core regions, transitioning into a [101] texture along the surfaces. The varied texture from core to surface validated the plastic strain FEM simulations, which predicted the presence of strain gradients across the wall thickness.

The consistent texture profile between both extrudates implied that an increase in exit speed had no significant effect on the resultant microstructural orientation. But, without a clear difference in exit temperature between both profiles, an assumption cannot be made if it has any effect on the resultant texture. Overall, EBSD proved to be sensitive to local deformation conditions, detecting differences between the core and surfaces of the extrudate and can be used for the analysis of extrudate quality.

References

[1] Sheppard, Extrusion of Aluminum Alloys, Kluwer Academic Publishers, Norwell. T., 1999. http://dx.doi.org/10.1007/978-1-4757-3001-2

[2] N. Biba, S. Stebunov, A. Lishny, The Model for Coupled Simulation of Thin Profile Extrusion, Key Eng. Mater. 504 (2012) 505-510. https://doi.org/10.4028/www.scientific.net/KEM.504-506.505

[3] W. Van Geertruyden, S. Claves, W.Z. Misiolek, Electron Backscatter Diffraction Analysis of Microstructural Evolution in Hot-Deformed 6xxx Series Aluminum Alloys, Metall. Mater. Trans. A. 33 (2002) 693-700. https://doi.org/10.1007/s11661-002-0132-3

[4] K. Rajan, Representations of Texture in Orientation Space, in: A.J. Schwartz, M. Kumar, B. L. Adams, D.P. Field (Eds.), Electron Backscatter Diffraction in Materials Science. New York: Springer, 2, 2009, pp. 31-38. https://doi.org/10.1007/978-1-4757-3205-4_3

[5] K. Rajan, Fundamentals of Automated EBSD, in: A.J. Schwartz, M. Kumar, B.L. Adams, D.P. Field (Eds.), Electron Backscatter Diffraction in Materials Science. New York: Springer, 2, 2009, pp. 51-64. https://doi.org/10.1007/978-1-4757-3205-4_5

[6] J. Zasadzinski, A. Rekas, W. Libura, D. Lesniak, Numerical Analysis of Aluminum Alloys Extrusion Through Porthole Dies, Key Eng. Mater. 424 (2010) 105-111. https://doi/org/10.4028/www.scientific.net/KEM.424.105

[7] P.P. Camus, S.I. Wright, M.M. Nowell, R. de Kloe, Scientific Analysis of NPAR Processing of EBSD Results for Beam-Sensitive Materials, Microscop. Microanal. 23 (2017) 1836-1837. https://doi.org/10.1017/S1431927617009849

[8] S.I. Wright, M.M. Nowell, S.P. Lindeman, P.P. Camus, M. De Graef, M.A. Jackson, Introduction and comparison of new EBSD post-processing methodologies, Ultramicroscopy 159 (2015) 81-94. https://doi.org/10.1016/j.ultramic.2015.08.001

[9] A.R. Eivani, J. Zhou, J. Duszczyk, Mechanism of the formation of peripheral coarse grain structure in hot extrusion of Al-4.5Zn-1Mg, Philos. Mag. 96 (2016) 1188-1196. https://doi.org/10.1080/14786435.2016.1157637

[10] W.H. Van Geertruyden, H.M. Browne, W.Z. Misiolek, P.T. Wang, Evolution of surface recrystallization during indirect extrusion of 6xxx aluminum alloys, Metall. Mater. Trans. A 36 (2005) 1049-1056. https://doi.org/10.1007/s11661-005-0298-6